Characterization of the corneal endothelial mosaic and comparison with simulated tessellations modeled with Gaussian random fields

Klervi Rannou, Yann Gavet, Jean-Charles Pinoli

Characterization of the corneal endothelial mosaic and comparison with simulated tessellations modeled with Gaussian random fields

Klervi Rannou[a], Yann Gavet[a], Jean-Charles Pinoli[a]
[a]École Nationale Supérieure des Mines de Saint-Étienne, LGF UMR CNRS 5307, 158 cours Fauriel, CS 62362, 42023 Saint-Étienne, France

ABSTRACT

In this article, manually segmented corneal endothelial mosaic will be characterized with spatial statistical functions and criteria issued from granulometry and morphometry. A novel approach to simulate spatial tessellations with Gaussian random fields with Gaussian and Bessel covariance functions, watershed and h-maxima is reported. Finally, these random spatial tessellations will be characterized and compared to corneal mosaics.

Keywords : corneal endothelial mosaic, simulated tessellations, Gaussian random fields, spatial statistical functions, granulometry, morphometry, shape diagrams

1 INTRODUCTION

The cornea is the transparent part of an eye in contact with the outside. Its role is to refract the light toward the retina. The cornea is made of different layers, the epithelium in contact with the outside, the Descemet membrane, the stroma and the endothelium.

The human corneal endothelium is a monolayer of space-filling flat hexagonal cells, which do not regenerate and are responsible for the maintenance of the cornea transparency. During the first years of life, the human corneal endothelial mosaic is a nearly regular hexagonal tessellation. But, with corneal growth and corneal diseases, the endothelial mosaic becomes less regular both in shape and size. Ophthalmologists need to have more knowledge about the endothelium, and above all about the cell density and morphology, to control in a better way grafts and disease evolution.

In this article, manually segmented corneal mosaic will then be characterized with criteria issued from granulometry and morphometry, and then compared to simulated tessellations obtained as realizations of Gaussian random fields.

2 MOSAIC CHARACTERIZATION

To compare corneal mosaics, and to simulate tessellations, some statistical information are needed. A tessellation (or mosaic) is the coverage of a region $D \subset \mathbb{R}^2$ by a countable set of regions $C_i \subset D$ such that for all $i \neq j$, $C_i \cap C_j = \emptyset$ and $\cup_i C_i = D$.

2.1 Centroid spatial distribution

To analyse the cell diameter and spatial distribution, the spatial distribution of their centroid is studied with the Ripley L function[12], the spherical contact distribution function F (also known as the empty space function or the point-event distance function) and the nearest-neighbour function G[5] (also named event-event function).

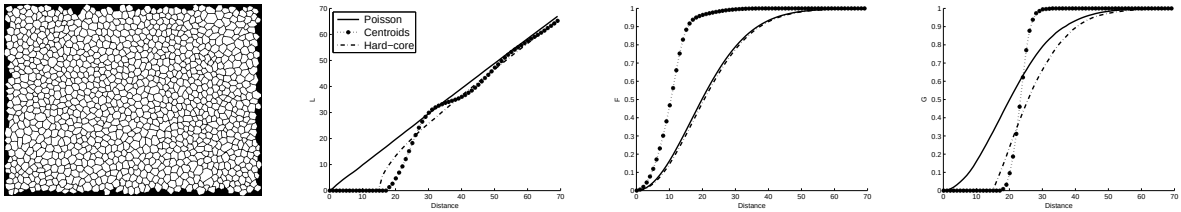

(a) (b) (c) (d)

Figure 1: Manually segmented corneal mosaic (a), and the statistical functions L (b), F (c), and G (d).

Let d be a distance over $T \subset \mathbb{R}^2$. Let P be a stationary point process on T, here it will be the cell centroids. Ripley's K function (reduced second moment function) of P is given, for all $t \in \mathbb{R}^+$, by:

$$K(t) := \frac{\mathbb{E}\left[\sum_{x \in T \cap B_\sigma(t)} N\left(\left(B_\sigma(t) + x\right) \setminus x\right)\right]}{\beta \mathbb{E}\left[N\left(T\right)\right]},$$

where $B_\sigma(t)$ is the open ball of radius t centred at the spatial origin $\sigma \in T$, $\forall A \subset T$, $N(A)$ is the number of points of P belonging to A, and β is the intensity of P given by $N(T) = \beta \times Area(T)$. Ripley's L function is given, for all $t \in \mathbb{R}^+$, by:

$$L(t) := \sqrt{\frac{K(t)}{\pi}}.$$

The spherical contact distribution function F of the point process P is given, for a fixed $u \in A \subset \mathbb{R}^2$ and for all $t \in \mathbb{R}^+$, by:

$$F(t) := \mathbb{P}\left[d(u, P) \leq t\right],$$

where:

$$\forall A \subset \mathbb{R}^2,\ d(u, A) := \min_{b \in A} \|u - b\|_2.$$

The nearest-neighbour function G of the point process P on $B \subset \mathbb{R}^2$ is given, for $u \in B$ and for all $t \in \mathbb{R}^+$, by:

$$G(t) := \mathbb{P}_{!u}\left[d(u, P) \leq t\right],$$

where $\mathbb{P}_{!u}$ is the reduced Palm distribution of $P \setminus \{u\}$ at u which can be seen as the conditional probability on the process P given that there is a point of P at u[7]. By stationarity assumption, G does not depend on u.

2.2 Centroid distribution of the corneal mosaic

These three functions of a manually segmented corneal mosaic are compared to the ones of a stationary Poisson process and a stationary Matérn hard core point process of type II[8] (Figure 1).

There is no cells of diameter lower to $t^* = 17.5$ for the reference mosaic Figure 1a (the L and the G functions are null for $t < t^*$).

2.3 Granulometry

The polymegathism (i.e. size variability) of endothelial cells interest the ophtalmologists. The area and perimeter kernel density estimate[9] of endothelial cells are hence computed (Figure 2), and are non-Gaussian.

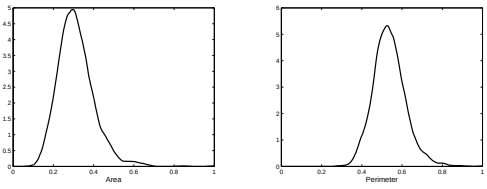

(a) Area (b) Perimeter

Figure 2: Area and perimeter kernel density estimate of a manually segmented corneal mosaic.

2.4 Morphometry

2.4.1 Shape diagrams

Ophthalmologists are also concerned by the pleomorphism (i.e. shape variability) of cells. Shape diagrams[13,14] are then studied. Shape diagrams are cloud point representations of the morphology of compact sets. The coordinate axes of the shape diagram are morphometrical functionals defined as ratios of geometrical functionals acting on the considered compact sets.

The considered geometrical functionals are the area A, the perimeter P, the radii of the inscribed and circumscribed circles (r and R), and the minimum and maximum Feret diameters (w and d).

The two shape diagrams used here are[14–16]:

- $\mathcal{D}_1$ which has w/d (diameter variation) as $x-$coordinate and $4A/\pi d^2$ (roundness) as $y-$coordinate,
- $\mathcal{D}_2$ which has $2\pi r/P$ (circularity) as $x-$coordinate and $4R/P$ (thinness) as $y-$coordinate.

For the manually segmented mosaic, each cell is mapped onto the diagrams $\mathcal{D}_1$ and $\mathcal{D}_2$ successively (Figure 3).

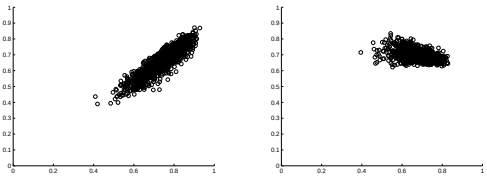

(a) $\mathcal{D}_1$ (b) $\mathcal{D}_2$

Figure 3: Shape diagrams $\mathcal{D}_1$ and $\mathcal{D}_2$ of the manually segmented endothelial mosaic.

2.4.2 Shape diagrams comparison

The root-mean-squared distance (RMSD) is computed on those shape diagrams to characterize the amount of dispersion of points around the centroid of the shape diagram, that is to say the shape homogeneity of the mosaic cells.

Let $(\mathbf{x}, \mathbf{y}) = \{(x_1, y_1), \ldots, (x_N, y_N)\}$ be the coordinates of N points of the shape diagram. The root-mean-squared distance of $(\mathbf{x}, \mathbf{y})$ is given by:

$$RMSD(\mathbf{x}, \mathbf{y}) = \sqrt{\frac{1}{N-1}\sum_{i=1}^{N}(x_i - \bar{x})^2(y_i - \bar{y})^2},$$

where $\bar{\mathbf{x}}$ is the mean of the vector $\mathbf{x}$.

Moreover, the RMSD of the reference endothelial mosaic is 0.118 for the first shape diagram $\mathcal{D}_1$, and 0.070 for the second one $\mathcal{D}_2$.

In the following, all these characteristics of the manually segmented endothelial mosaic (Figure 1a), will be compared to the characteristics employed in a novel approach to obtain random spatial tessellations.

3 MOSAIC SIMULATION

3.1 Random fields

To simulate tessellations, the first used tool is a random field. Most definitions and results about random fields come from [1–3,11,18].

A random field X_t associates to each point t of a topological space $T \subset \mathbb{R}^2$ a real random variable which depends of its neighbourhood field values. These values could also be seen as heights and a random field may thus be viewed as an hyper-surface. In this work the random fields will be Gaussian, separable, stationary and isotropic.

To simulate a Gaussian random field, the only think needed is a covariance function. In this work, two covariance functions will be used: the Gaussian and the Bessel ones. For all $\tau \geq 0$ (τ designate the distance between points of the space T), the Gaussian covariance function C_G is given by:

$$C_G(\tau) = \exp\left(-\frac{\tau^2}{2l^2}\right),$$

where $l \geq 0$ is the correlation length, and the Bessel covariance function C_B is given by:

$$C_B(\tau) = \begin{cases} 2^\nu \Gamma(\nu+1) \left(\frac{\tau}{l}\right)^{-\nu} J_\nu\left(\frac{\tau}{l}\right) & \text{if } \tau > 0, \\ 1 & \text{if } \tau = 0, \end{cases}$$

where $l \geq 0$ is the (angular) period, Γ is the gamma function (or Euler integral of the second kind), and J_ν is the Bessel function for $\nu \geq 0$.

3.2 Generalized Voronoï diagram

To simulate tessellations, germs that will be the nuclei of the cells are needed. The germs will be the local maxima or h-maxima locations of Gaussian random field realizations. The definition of this kind of maximum come from mathematical morphology [17]

Let h be a non-negative real number. A point z of X belongs to an h-maximum if and only if z doesn't belong to the mathematical reconstruction of X by $X - h$. If $h = 0$, the h-maximum is called local maximum. The orthogonal projection of the h-maxima over T will be called extended h-maxima.

They are several ways to obtain tessellations from germs. The most widely used is the Voronoï diagram [4], it could be used only with local maxima's. Some cells of the tessellation obtained with the Voronoï diagram are too small, because the inter-point distance between local maxima's could be very small.

This way to obtain tessellation cannot be used with extended h-maxima, for $h > 0$, because extended h-maxima are compact and connected sets. A generalization of the Voronoï diagram is then used with such germs named skeleton by influence zone or SKIZ [6].

The steps to obtain a tessellation from a realization of a Gaussian random field, his extended h-maxima and the related SKIZ are shown in Figure 4.

4 MOSAIC COMPARISON

The manually segmented endothelial mosaic Figure 1a is now compare to tessellations simulated with the SKIZ of realizations of Gaussian random fields with Gaussian and Bessel covariance functions.

4.1 Spatial distribution functions

In Figure 5, the L, F and G functions of the local maxima and centroids of tessellations cells obtained by the SKIZ of realizations of Gaussian random fields with Gaussian and Bessel covariance functions are added to the ones of Figure 1. As expected, the distance between local maxima could be close to zero, whereas with the use of the SKIZ, i.e. of h-maxima with a non-null h, there is no too small-size cells. This confirm the choice of using h-maxima and the SKIZ rather than local maxima and the Voronoï diagram. Furthermore, the statistical functions of simulated tessellations with the Bessel covariance function are closer to the corneal mosaic.

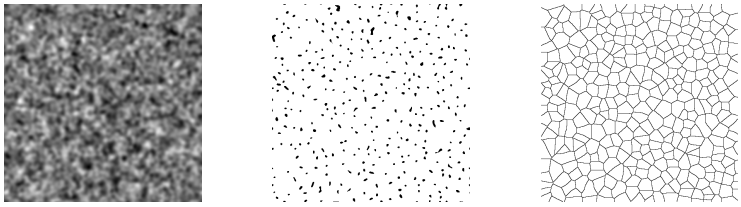

(a) Field realization (b) Extended h-maxima (c) SKIZ

Figure 4: Steps in the simulation of a tessellation from (a) a realization of a Gaussian random field, here, with a Gaussian covariance function. (b) First the extended h-maxima are found, and (c) next the tessellation is obtained with the SKIZ.

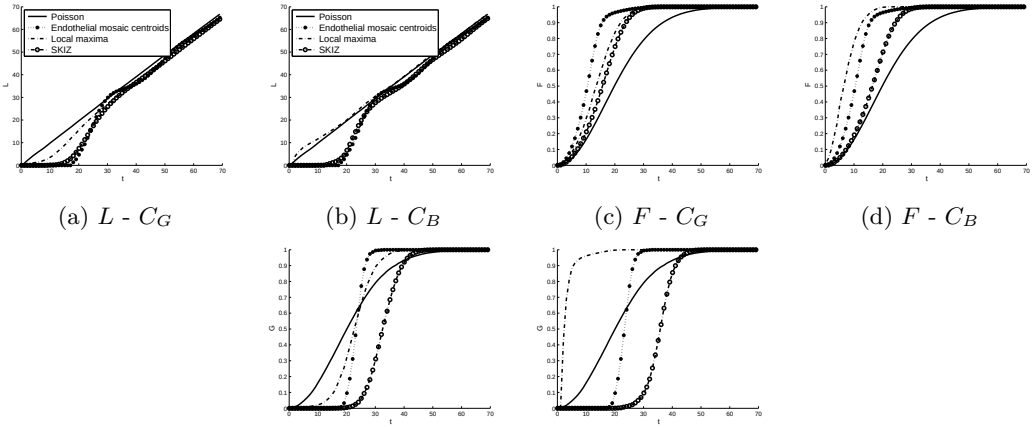

(a) L - C_G (b) L - C_B (c) F - C_G (d) F - C_B

(e) G - C_G (f) G - C_B

Figure 5: The L (a,b), F (c,d) and G (e,f) function for a stationary Poisson process, the reference endothelial mosaic, the local maxima and the SKIZ cells centroids of realizations of Gaussian random fields with Gaussian C_G (a,c,e) and Bessel C_B (b,d,f) covariance functions.

4.2 Granulometry

To compare area and perimeter kernel density estimate (Figure 6), two histogram distance[10] function will be used, the Chi-Squared (χ^2) histogram distance function which is a bin-to-bin distance function and the Quadratic-Chi histogram distance function (QC_m) which is a cross-to-bin distance function.

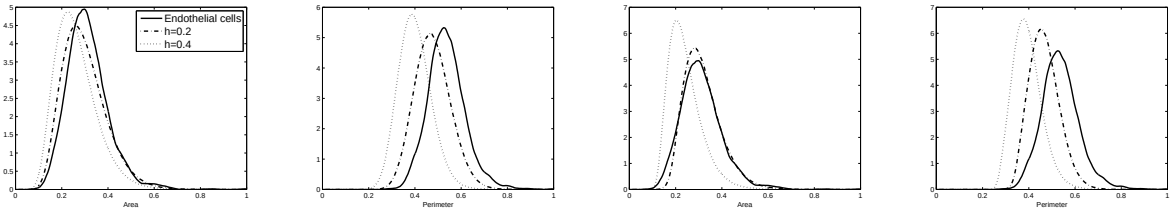

(a) Area - C_G (b) Perimeter - C_G (c) Area - C_B (d) Perimeter - C_B

Figure 6: Area and perimeter kernel density estimate for the endothelial mosaic, and 10^6 tessellation cells obtained with the SKIZ method for various h and realization of Gaussian random fields with a Gaussian C_G and a Bessel C_B covariance function.

Let P and Q be two non-negative bounded histograms, which bins are intervals $\left[\frac{i}{k}, \frac{i+1}{k}\right[\subset [0,1[$, $k \in \mathbb{N}^*$.

The Chi-Squared histogram distance function is:

$$\chi^2(P,Q) = \frac{1}{2}\sum_i \frac{(P_i - Q_i)^2}{P_i + Q_i}.$$

Let A be a matrix defined by:

$$\forall i,j \in \{1,\ldots,k\}, A_{ij} := 1 - \frac{d(x_i,x_j)}{\max_{i,j} d(x_i,x_j)},$$

where d is a distance function on $[0,1]$. Let $0 \leq m < 1$. The Quadratic-Chi histogram distance function is:

$$QC_m(P,Q) := \sqrt{\sum_{i,j}\left(\frac{(P_i - Q_i)}{\left(\sum_c (P_c + Q_c)A_{c_i}\right)^m}\right)\left(\frac{(P_j - Q_j)}{\left(\sum_c (P_c + Q_c)A_{c_j}\right)^m}\right)A_{ij}}.$$

The two distances, Figure 7, indicate that the perimeter and area histograms of simulated tessellations are closer to the endothelial ones for h between 0.05 and 0.2 for the Gaussian covariance function, and between 0.15 and 0.2 for the Bessel one.

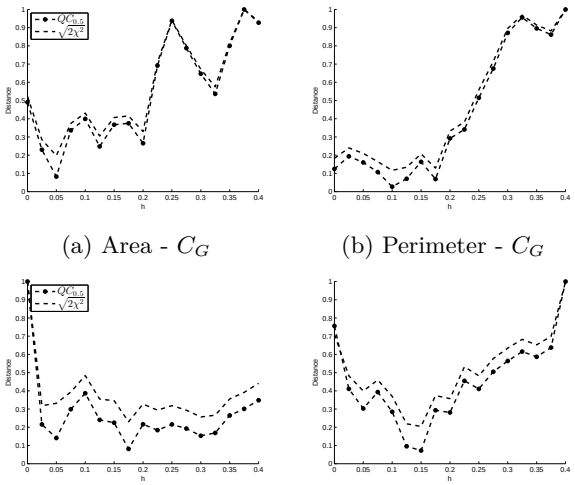

(a) Area - C_G (b) Perimeter - C_G

(c) Area - C_B (d) Perimeter - C_B

Figure 7: Comparison, with the Chi-Squared χ^2 and the Quadratic-Chi QC_m histogram distance, between area and perimeter kernel density estimate of endothelial cells and 10^6 tessellation cells obtained with the SKIZ method for various h and realizations of Gaussian random fields with a Gaussian C_G and a Bessel C_B covariance function, respectively.

4.3 Morphometry

The aim here is to identify which shape diagram of tessellations simulated with the SKIZ of realizations of Gaussian random fields with Gaussian and Bessel covariance functions is closer in terms of centroid and shape to that of endothelial cells.

First, the RMSD of the shape diagrams of simulated tessellations is computed table 1. The cells simulated with a Bessel covariance present more homogeneity in shape than the ones simulated with a Gaussian covariance, and is closer to the RMSD obtained for the endothelial tessellation with $h = 0.15$.

Moreover, to analyse the spatial homogeneity of cells, two others criteria are studied, the Euclidean distance between the centroids of the shape diagrams and the Fréchet-Nikodým distance between dilated shape diagrams.

Table 1: Root-mean-squared distance ($RMSD$) of shape diagrams of simulated cells obtained from the h-maxima transform of Gaussian random fields with Bessel and Gaussian covariance with different h.

h	Bessel covariance		Gaussian covariance	
	$\mathcal{D}_1$	$\mathcal{D}_2$	$\mathcal{D}_1$	$\mathcal{D}_2$
	$RMSD$	$RMSD$	$RMSD$	$RMSD$
0	0.252	0.182	0.157	0.094
0.05	0.170	0.110	0.146	0.086
0.1	0.128	0.074	0.146	0.086
0.15	**0.127**	**0.070**	0.148	0.085
0.2	0.128	0.071	0.146	0.083
0.25	0.131	0.073	0.150	0.087
0.3	0.130	0.072	0.147	0.085

The Fréchet-Nikodỳm distance (or symmetric-difference distance) between two Lebesgue measurable subsets A and B of T is given by:

$$d_\Delta(A,B) := \mu(\Delta(A,B)),$$

where μ is the Lebesgue measure on T and Δ is the symmetric difference operator:

$$\begin{aligned}\Delta(A,B) &= (A \cup B) \setminus (B \cap A) \\ &= (A \setminus B) \cup (B \setminus A).\end{aligned}$$

Results are presented in table 2. One more time, simulated cells obtained from Gaussian random fields with a Bessel covariance function are closer to endothelial cells regarding their morphometrical characteristics than cells simulated with a Gaussian covariance function.

Table 2: Euclidean distance (δ) and Fréchet-Nikodỳm distance d_Δ between centroids of shape diagrams of endothelial and simulated cells. Simulated cells are obtained from the $h-$maxima transform of Gaussian random fields with Bessel and Gaussian covariance with different h values. The more interesting results are highlighted in bold.

h	Bessel covariance				Gaussian covariance			
	$\mathcal{D}_1$		$\mathcal{D}_2$		$\mathcal{D}_1$		$\mathcal{D}_2$	
	δ	d_Δ	δ	d_Δ	δ	d_Δ	δ	d_Δ
0	0.199	0.506	0.176	0.507	0.102	0.367	0.099	0.331
0.05	0.069	0.380	0.072	0.379	0.088	0.327	0.084	0.284
0.1	**0.044**	0.260	**0.048**	0.227	0.092	0.315	0.084	0.270
0.15	0.051	0.244	**0.048**	0.216	0.090	0.320	0.081	0.261
0.2	0.054	0.244	0.051	0.209	0.094	**0.296**	0.080	**0.260**
0.25	0.063	**0.243**	0.054	**0.187**	0.100	0.326	0.084	0.291
0.3	0.068	0.251	0.056	0.216	0.100	0.311	0.080	0.297

5 CONCLUSION

The novel mathematical approach used to simulate random spatial tessellations gives more variability in shapes and sizes of cells than the methods used up to now. With this approach, the Bessel covariance function is the best, amongst the ones studied in this article, to simulate tessellations close to the corneal mosaic. The choice of the optimal value for the h parameter is not obvious, the different criteria of the present granulometric and morphometric study gives an h value lying between 0.1 and 0.25. Other random fields and covariance functions will be tested and used. Other manually segmented corneal endothelial mosaic at different time of life and different pathologies will be characterized.

ACKNOWLEDGMENTS

This research was supported by a grant: ANR-12-TECS-004, CorImMo 3D, TecSan 2012. The authors wish to thank Pr. Gilles Thuret and Pr. Philippe Gain from the BiiGC, University Jean Monnet, Saint-Etienne, France, for providing pictures of the human corneal endothelium.

References

[1] Abrahamsen, P., [A review of Gaussian random fields and correlation functions], Norsk Regnesentral/Norwegian Computing Center, (1997)

[2] Adler, R. J., [The geometry of random fields], Siam, (1981)

[3] Adler, R. J. and Taylor, J. E., [Random fields and their geometry], Birkhäuser, Boston, (2005)

[4] Aurenhammer, F. and Klein, R., "Voronoi diagrams", Handb. Comput. Geom. , 5, 201–290, (2000)

[5] Baddeley, A., "Spatial point processes and their applications", Springer Verlag, (2006)

[6] Beucher, S. and Lantuejoul, C., "Use of watersheds in contour detection", Proc. International Workshop on Image Processing, Real-Time Edge and Motion Detection/Estimation, Rennes, (1979)

[7] Cressie, N., "Statistics for spatial data", Terra Nova, 4(5), 613–617, (1992)

[8] Matérn, B. and others, "Spatial variation. Stochastic models and their application to some problems in forest surveys and other sampling investigations", Meddelanden fran statens Skogsforskningsinstitut, 49(5), (1960)

[9] Parzen, E., "On estimation of a probability density function and mode", The annals of mathematical statistics, 1065–1076, (1962)

[10] Pele, O. and Werman, M., "The quadratic-chi histogram distance family", Computer Vision–ECCV 2010, 749–762, (2010)

[11] Rasmussen, C. E., "Gaussian processes for machine learning", MIT Press, (2006)

[12] Ripley, B. D., "Modelling spatial patterns", J. R. Stat. Soc. Ser. B Stat. Methodol., 39(2), 172-212, (1977)

[13] Rivollier, S., Debayle, J. and Pinoli, J.-C., "Shape representation and analysis of 2d compact sets by shape diagrams", Image Processing Theory Tools and Applications (IPTA), 2010 2nd International Conference on, 411–416, (2010)

[14] Rivollier, S., Debayle, J. and Pinoli, J.-C., "Shape diagrams for 2d compact sets-Part I: analytic convex sets", Aust. J. Math. Anal. Appl., 7(2), (2010)

[15] Rivollier, S., Debayle, J. and Pinoli, J.-C., "Shape diagrams for 2d compact sets-Part II: analytic simply connected sets", Aust. J. Math. Anal. Appl., 7(2), (2010)

[16] Rivollier, S., Debayle, J. and Pinoli, J.-C., "Shape diagrams for 2d compact sets-Part III: convexity discrimination for analytic and discretized simply connected sets", Aust. J. Math. Anal. Appl., 7(2), (2010)

[17] Soille, P., [Morphological image analysis: principles and applications], Springer, (2003)

[18] Yaglom, A. M., [Correlation theory of stationary and related random functions], Springer, (1987)